# Design of Single Narrow Band Bandpass Filter using Cascaded Open Loop Triangular Ring Resonators Embedded with Rectangular Ring

Yatindra Gaurav and R. K. Chauhan
*Department of Electronics and Communication Engineering, Madan Mohan Malaviya University of Technology, Gorakhpur, Uttar Pradesh, India.*
*ygaurav2000@gmail.com*

***Abstract*—This paper presents a compact single narrow band bandpass filter using two cascaded open loop triangular ring resonator embedded with rectangular ring for various application at 11.8 GHz in microwave communication systems. Coupled resonator theory was used for coupling parasitic resonance of multiple degenerate modes operating close to the fundamental mode in the proposed structure of filter. The frequency response has low insertion loss and good rejection performance of the proposed filter. The filter was easy to fabricate since there was no use of via or defected ground structure. Cascading and the embedded rectangular ring were used to improve the stop band performances by creating several attenuation poles. A wide stop band was obtained at both the sides of passband. The proposed filter was designed and simulated in Agilent Advance Design System. The simulated result and the measured results were in good agreement.**

***Index Terms*—Cascaded Structures; Narrow Band Bandpass Filter; Open Loop Triangular Ring Resonator; Rectangular Ring Resonator and Selectivity.**

## I. Introduction

High performance microwave filters with compact size has influenced the wireless communication systems. Resonators are the fundamental element for designing microstrip filters [1-7]. Resonator size is the main constraint in designing part since it determines the size of filter. Reduction in size of resonator will reduce the size of filter. To reduce the size of the filter, the resonator structure or the traditional resonator is modified so that additional modes can be created, which further improves the performance of the filter since it works as a multimode resonator [8-10].

Modified resonator can be treated as multiple electrical resonators. Filters design by multimode resonators has relatively low insertion loss and compact size. Coupling among the degenerate modes is the challenging issue in designing of filters with high performance using single multimode resonators when compared with multiple multimode resonators since parasitic resonances of multiple degenerate modes operate close to fundamental mode [11-21]. To design a filter with single multimode resonator with high rejection performance is a challenging issue and continuous effort is given by researchers to overcome it.

In this paper, a single band bandpass filter using cascaded open loop triangular ring resonator embedded with rectangular ring is presented. The filter, with low insertion loss, provides one transmission bands. The dielectric material that is being used in designing the proposed filter is Rogers RT Duroid 6010 with dielectric constant as 10.2 and thickness as 1.27 mm.

## II. Design Of Single Narrow Band Bandpass Filter

An effective approach is adopted to design a filter by single multimode resonator with wide stop band on both the sides of passband using Open loop triangular ring resonator. Triangular resonator is used in the design since it has small size when compared to conventional resonators.

Figure 1 shows the conventional design of closed loop triangular ring resonator as dual-mode bandpass filter. Different types of responses with different position and sizes of perturbation can be obtained for bandpass filter. According to resonant mode theory and slow-wave effect, triangular patch function is equal to cutting a part of the structure that introduces a change in field distribution and inspires the degenerate modes, which further generates attenuation poles due to cross coupling of it with a shift of resonant frequency of higher harmonic wave, achieving miniaturized filter design technique.

Figure 1: Configuration of the conventional triangular dual-mode filter

The fundamental resonance occurs when $\lambda_g$ is the perimeter of the outer equilateral triangle, where $\lambda_g$ is the guided wavelength.

$$\lambda_g = \frac{c}{f\sqrt{\varepsilon_{eff}}} \qquad (1)$$

where: c = the velocity of light in free space
$\varepsilon_{eff}$ = effective dielectric constant of the substrate
f = resonant frequency

While a resonant frequency is fixed, $\lambda_g$ is decreased to realize size reduction as $\varepsilon_{eff}$ increased. Similarly, for a fixed $\varepsilon_{eff}$, the resonant frequency f is decreased as the perimeter increased.

An open-loop resonator has an important role in couplings with transmission line with loaded stubs in the structure. The coupling strength and its characteristics are not only determined by the nature and extent of the field along the resonator but also the length and width of the side of triangular ring resonator. Coupling coefficient of open loop triangular ring resonator can be characterized by its dimension and the relative dielectric constant $\varepsilon_r$ for a given substrate with a thickness h. Open loop resonator encounters both electric coupling and magnetic coupling, giving better coupling and lower insertion loss.


Figure 2: Structure of open loop triangular ring resonator coupled in series with transmission line.

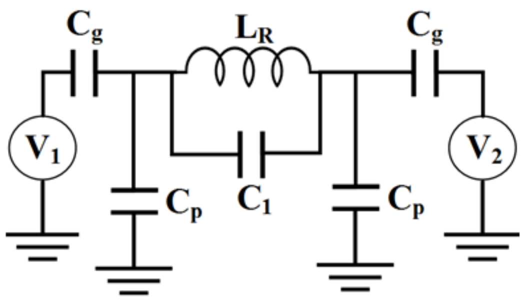


Figure 3: Structure of open loop triangular ring resonator coupled in series with transmission line.

Figure 2 shows the structure of open loop triangular ring resonator coupled with transmission line in series. Figure 3 shows the equivalent circuit of the open loop triangular ring resonator coupled with transmission line. $L_R$ represents the inductance due to length of resonator, $C_1$ represents the capacitance due to slot in the ring to make it open, $C_P$ is the parasitic capacitance due to the dielectric used and $C_g$ is the coupling capacitance due to the port. When an open loop triangular ring resonator is coupled in series with transmission line, a passband is seen in the s-parameter characteristics. Figure 4 shows the resonant frequency as given by Equation (2).

$$f_o = \frac{c}{2L\sqrt{\varepsilon_{eff}}} \tag{2}$$

where: c = speed of light.
$f_o$ = fundamental resonant frequency.
L = total length of microstrip line in open loop triangular ring resonator and comprises $L_2$ as one of its part.
$\varepsilon_{eff}$ = effective dielectric constant.

The resonant frequency of a resonator depends on its electrical length $\lambda_g/2$; therefore, Length $L_2$ determines its resonant frequency. For required resonating frequency, L is calculated. $L_3$ is the length of coupling that decides the coupling capacitor ($C_g$). The resonant frequency is centered at 8 GHz for satellite communication. A wide Stopband is achieved on both side of passband. The insertion loss and return loss in passband is 1.1 dB and 18.7 dB. The selectivity at the passband edges is achieved. An upper stopband extends from 18.2 GHz to 18 GHz with return loss less than 3 dB and maximum value of insertion loss as 29 dB is obtained, as shown inFigure 4.

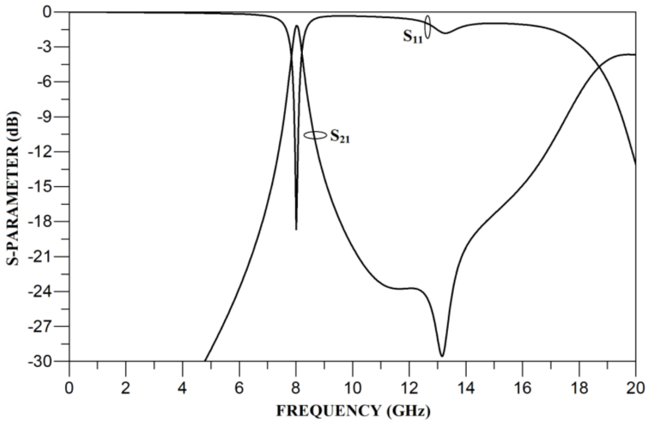


Figure 4: Frequency response of open loop triangular ring resonator coupled in series with transmission line.

To improve the insertion loss and selectivity of Figure 4, two triangular open loop resonators are cascaded to form pseudo hexagonal closed loop resonator, as shown in Figure 5. The modification in hexagonal closed loop resonator generates some capacitive effects like $C_2$ as shown in its equivalent circuit. The value of $C_2$ depends on the dimensions of $L_1$ and $L_4$, as shown in Figure 5 and Figure 6. The equivalent circuit of the pseudo hexagonal resonator indicates that this resonator will resonate at two frequencies and it is verified in simulated result as shown in Figure 9. The resonating frequencies of the proposed filter are dependent on the dimensions of $L_1$, $L_2$, $L_4$, $W_2$ and $W_3$. On decreasing length $L_4$ from 1.3 mm to 0.7 mm, the centre frequency of first passband increases with the increase in return loss while the insertion loss remains almost constant. The second passband centre frequency also shifts towards higher frequency side with degradation in the value of insertion loss, see Figure 7. On varying the length $L_1$ , it was found that the second passband is more affected than first passband. The insertion loss of second pass band is improved on decreasing length $L_1$ (see Figure 8). This is due to the fact that effective capacitance of the cascading structure forming the close loop increases with the increase in length $L_1$. To achieve the required passband performance with respective resonance frequency and the band rejection performance, length $L_1$ and $L_4$ are optimized. The two passbands centered at 7.77 GHz and 13.5 GHz are seen in the frequency response of the structure shown in Figure 5. The first passband has insertion loss as 0.621 dB and return loss as 27.6 dB. The second passband has insertion loss as 3.34 dB and return loss as 15.785 dB. The two passbands are separated by stop band that extends from 8.23 GHz to 12.7 GHz. The stop band has maximum value of insertion loss as 15.8 dB and minimum value of return loss as 0.5 dB. The upper stop band extends from 14.2 GHz with maximum insertion loss as 28 dB and returns loss less than 3 dB (See Figure 9).

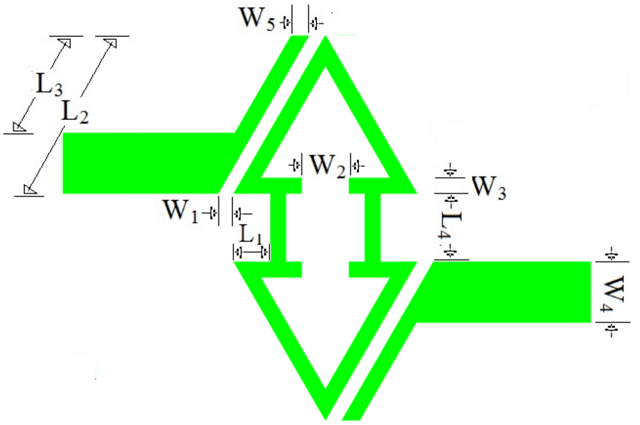


Figure 5: Structure of cascaded open loop triangular ring resonator loaded with stub.

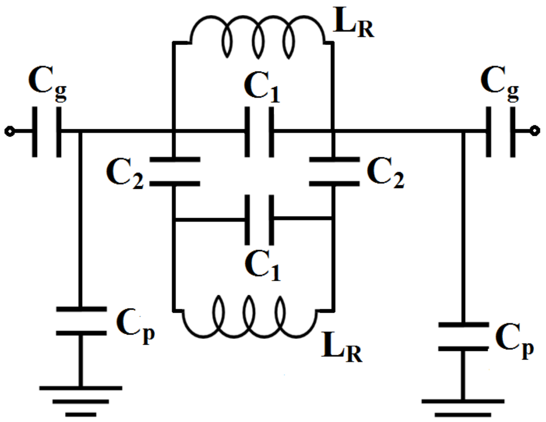


Figure 6: Equivalent circuit of cascaded open loop triangular ring resonator loaded with stub.

To improve the frequency response of the cascaded structure forming the closed loop and to have a single multimode resonator, resonating at required frequency, a rectangular ring is embedded to the above structure (See Figure 10). The electrical coupling at the open loop area of overall structure is improved due to which a single resonant frequency is obtained. According to coupled resonator theory, the field associated with the structure shown in Figure 5 is disturbed when the rectangular ring is embedded, inspiring degenerate modes which further generates attenuation poles; thus improving the selectivity of the filter with the creation of transmission zeros at the edges of the passband. This process subsequently improves the rejection performance of the filter with a shift of passband towards the lower frequency side. A comparative frequency response of proposed filter with and without rectangular ring is shown in Figure 11. A single passband is obtained in the frequency response of proposed filter centered at 11.8 GHz. The extra resonating frequency in the s-parameter performance of the proposed filter is due to the capacitive effects of $C_1$ and $C_2$ along with the inductor $L_R$ in the cascaded structure forming pseudo hexagonal ring. The value of insertion loss in the passband is 1.8 dB and return loss as 24.72 dB. The upper stop band extends from 12.3 GHz with return loss less than 1.7 dB and insertion loss more than 15 dB (See Figure 12).

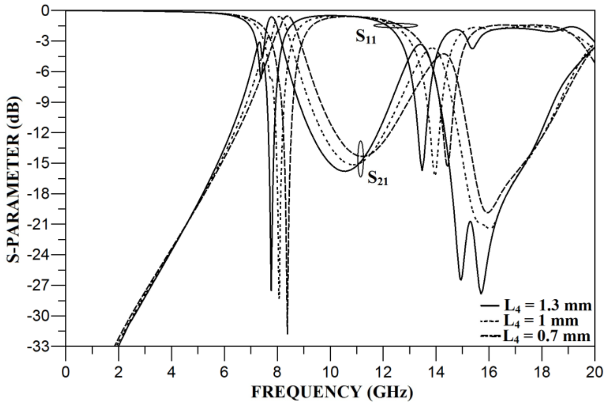


Figure 7: Frequency response of cascaded open loop triangular ring resonator with varied stub length L4.

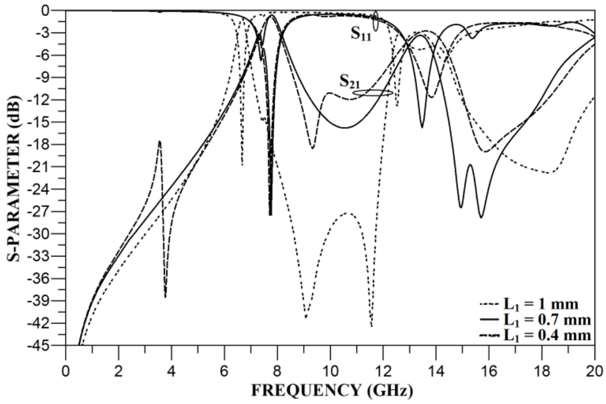


Figure 8: Frequency response of cascaded open loop triangular ring resonator with varied length L1

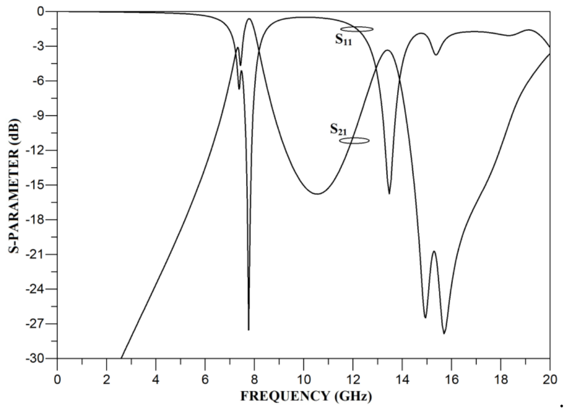


Figure 9: Frequency response of cascaded open loop triangular ring resonator loaded with stub.

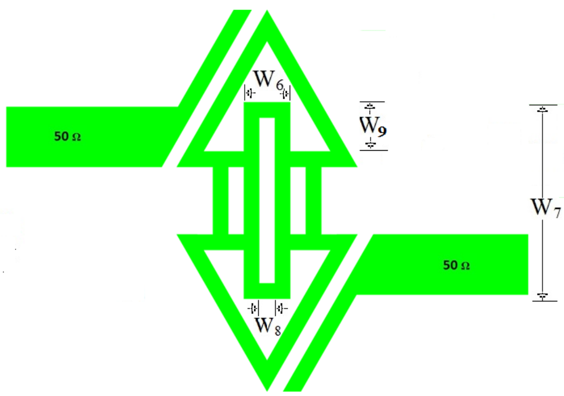


Figure 10: Structure of proposed filter.

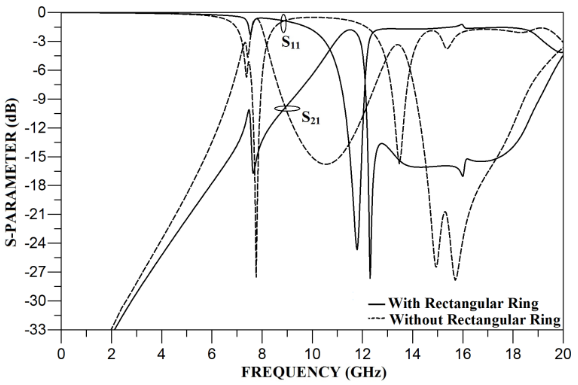


Figure 11: Comparative frequency response of proposed filter with and without rectangular ring.

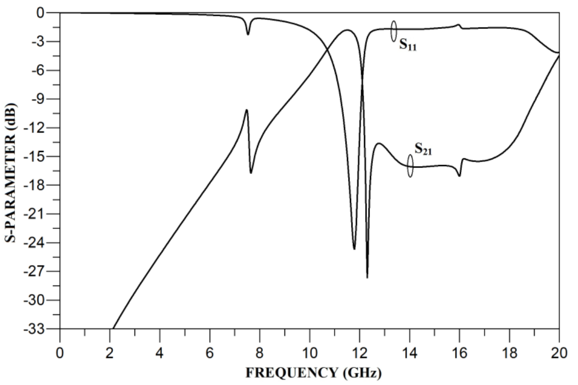


Figure 12: Frequency response of proposed filter.

## III. Fabrication And Measurement

The optimized dimensions of the proposed design are as follows: $L_1$ = 0.7 mm, $L_2$ = 3.5 mm, $L_3$ = 2.16 mm, $L_4$ = 1.3 mm, $W_1$ = 0.3 mm, $W_2$ = 0.9 mm, $W_3$ = 0.3mm, $W_4$ = 1.16 mm, $W_5$ = 0.35, $W_6$ = 0.9 mm, $W_7$ = 3.79 mm, $W_8$ = 0.3 mm and $W_9$ = 0.95 mm. The overall size of the fabricated filter is 7.36 mm x 3.5 mm. The photograph of the fabricated filter is shown in Figure 13. Frequency response of proposed structure has single passband centered at 11.8 GHz, whereas its measured value is the same. The simulated insertion loss and return loss of passband is 1.8 dB and 24.72 dB, whereas its measured results are 1.7 dB and 24 dB. The simulated upper stopband extends from 12.3 GHz and its counterpart is 12.25 GHz. The simulated insertion loss and return loss in upper stop band is more than 15 dB and less than 1.7 dB, whereas its measured results are less than 0.9 dB and more than 11.5 dB (See Figure 14).

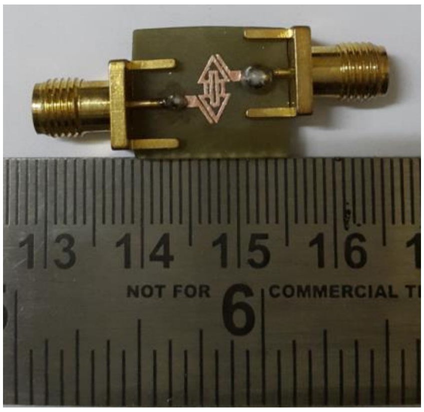


Figure 13: Photograph of the fabricated proposed Filter.

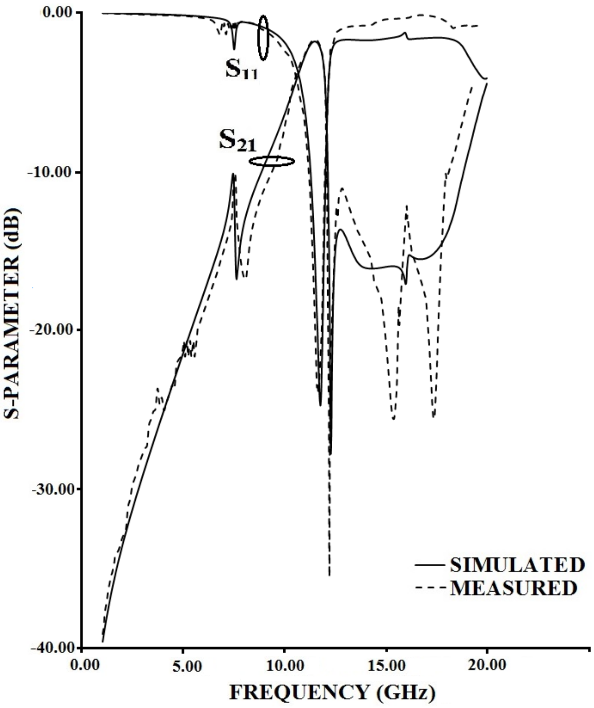


Figure 14: Simulated and measured Frequency response of the proposed filter.

## IV. Conclusions

A compact and planar single narrow band bandpass filter using two cascaded open loop triangular ring resonator embedded with rectangular ring is proposed. Frequency response clearly shows that coupled resonator theory is used for coupling parasitic resonance of multiple degenerate modes operating close to fundamental mode. The proposed structure generates single narrow passband centered at 11.8 GHz with 3 dB fractional bandwidth of 9.47%. A wide upper stop band is obtained that extends from 12.3 GHz. A good rejection performance with selectivity is obtained making it applicable in various microwave communication systems.

## References

[1] Y.C. Chiou and J.T. Kuo, "Planar multiband bandpass filter with multimode stepped-impedance resonators," *Progress In Electromagnetics Research*, vol. 114, pp. 129-144, 2011.

[2] X.G. Huang, Q.Y. Feng, and Q.Y. Xiang, "High selectivity broadband bandpass Filter using stub-loaded quadruple-mode resonator," *Journal of Electromagnetic Waves and Applications*, vol. 26, no. 1, pp. 34-43, 2012.

[3] L. Wang and B.R. Guan, "Compact and high selectivity dual- band bandpass filter using nested dual-mode defected ground structure resonators," *Journal of Electromagnetic Waves and Applications*, vol. 26, no. 4, pp. 549-559, 2012.

[4] J. R. Lee, J. H. Cho, and S. W. Yun, "New compact bandpass filter using microstrip $\lambda$/4 resonators with open stub inverter," *IEEE Microwave and Guided Wave Letters*, vol. 10, pp. 526-527, Dec. 2000.

[5] P. Mondal and M. K. Mandal, "Design of dual-band bandpass filters using stub-loaded open-loop resonators," *IEEE Trans. Microwave Theory Tech.*, vol. 56, pp. 150-155, Jan. 2008.

[6] Y. T. Kuo, "Analytical design of two-mode dual-band filters using E-shaped resonators," *IEEE Trans. Microwave Theory Tech.*, vol. 60, pp. 250-260, 2012.

[7] J.S. Hong, and M. J. Lancaster, *Microstrip Filters for RF/Microwave Applications*, John Wiley & Sons, Inc., 2001

[8] M. K. Sagawa, Takahashi, and M. Makimoto, "Miniaturized hairpin resonator filters and their application to receiver front end MIC's," *IEEE Trans. Microwave Theory Tech.*, vol. 37, pp. 1991-1996, 1989.

[9] K. Ma, K. S. Yeo, J.G. Ma, and M. A. Do, “An ultra- compact hairpin band pass filter with additional zero points," *IEEE Microwave and Wireless Components Lett.*, vol. 17, pp. 262-264, 2007.

[10] K. Ma, J.G. Ma, K. S. Yeo, and M. A. Do, “A compact size coupling controllable filter with separated electric and magnetic coupling paths," *IEEE Trans. Microwave Theory Tech.*, vol. 54, no. 3, pp. 1113-1119, 2006.

[11] I. Awai, A. C. Kundu, and T. Yamashita, “Equivalent- circuit representation and explanation of attenuation poles of a multimode dielectric-resonator bandpass filter," *IEEE Trans. Microwave Theory Tech.*, vol. 46, pp. 2159-2163, 1998.

[12] L.P. Zhu, Wecowski, and K. Wu, “New planar multimode filter using cross-slotted patch resonator for simultaneous size and loss reduction," *IEEE Trans. Microwave Theory and Tech.*, vol. 47, no. 5, pp. 650-654, 1999.

[13] J.S. Hong and M. J. Lancaster, “Microstrip triangular patch resonator filters," *IEEE MTT-S Int. Symp. Dig.*, pp. 331-334, 2000.

[14] L. Zhu, S. Sun, and W. Menzel, “Ultra-wideband (UWB) bandpass filters using multiple-mode resonator," *IEEE Microwave and Wireless Components Lett.*, vol. 15, no. 11, pp. 796-798, 2005.

[15] K. Ma, K. C. B. Leong, R. M. Jayasuriya, and K. S. Yeo, “A wideband and high rejection multimode bandpass filter using stub perturbation," *IEEE Microwave and Wireless Components Lett.*, vol. 19, pp. 24-26, 2009.

[16] H. Shaman and J.S. Hong, “A novel ultra-wideband (UWB) bandpass filter (BPF) with pairs of transmission zeroes," *IEEE Microwave and Wireless Components Lett.*, vol. 17, no. 2, pp. 121-123, 2007.

[17] L.H. Hsieh and K. Chang, “Compact elliptic-function low-pass ¯lters using microstrip stepped-impedance hairpin resonators," *IEEE Trans. Microwave Theory and Tech.*, vol. 51, no. 1, pp. 193-199, 2003.

[18] S.C. Bastioli, Tomassoni, and R. Sorrentino, “A new class of waveguide dual-mode filters using TM and nonresonating," *IEEE Trans. Microwave Theory and Tech.*, vol. 58, no. 12, pp. 3909-3917, 2010.

[19] Norfishah A. Wahab, M. K. M. Salleh, Sameh K. M. Khanfar, Zuhani I. Khan, and Zaiki Awang., “Synthesis of a single-side-access-ring resonator for higher order bandpass filters,” *Progress in Electromagnetic Research Letters.*, vol. 38, pp. 137-150, 2013.

[20] J. G. Zhou, Y.C. Chiang and W. Che., “Compact wideband balanced bandpass filter with high common-mode suppression based on cascade parallel coupled-lines,” *IET Microwaves, Antenna & Prop.*, vol. 18, pp. 564-570, 2014.

[21] W. Wang, Q. Cao, C. Yang, Y. Wang and Y. Chen., “Design of dual-bandpass filters using stepped-impedance circular ring resonator,” *Electronics Letters.*, vol. 51, no. 25, pp. 2117-2119, 2015.